



ELSEVIER

Available online at [www.sciencedirect.com](http://www.sciencedirect.com)

SCIENCE @ DIRECT®

Physica A 329 (2003) 41–52

PHYSICA A

[www.elsevier.com/locate/physa](http://www.elsevier.com/locate/physa)

# Time evolution of clusters of mobile particles in a model glass former

G.A. Appignanesi<sup>a,b,\*</sup>, M.A. Frechero<sup>a</sup>, R.A. Montani<sup>a</sup>

<sup>a</sup>*Departamento de Química, Universidad Nacional del Sur (UNS), Av. Alem 1253, Bahía Blanca 8000, Argentina*

<sup>b</sup>*Instituto de Matemática (INMABB-UNS-CONICET), Av. Alem 1253, Bahía Blanca 8000, Argentina*

Received 6 November 2002; received in revised form 13 February 2003

## Abstract

In this work we investigate by means of molecular dynamics simulations the detailed time evolution of string-like cooperative motions in a binary Lennard–Jones system at temperatures close to its mode-coupling temperature,  $T_c$ . The strings will be fully geometrically and dynamically characterised, making evident the correlated and concerted nature of the motions of the particles comprised. We shall show that at low temperature each string occurs in a sharp time window within the time interval  $[0, t^*]$ , where  $t^*$  is a characteristic time related to the lifetime of the global clusters of mobile particles. Moreover, the different strings that comprise a given global cluster will be shown to take place independently and asynchronously, thus providing further support to the heterogeneous scenario of relaxation, but in which different independent string-like sub-regions relax at different timescales. Finally, we shall also demonstrate that as temperature is increased the strings evolve during an increasing fraction of the time interval  $[0, t^*]$  and that for  $T \sim 0.55$  the lifetimes of the strings and of the global clusters become akin to each other.

© 2003 Elsevier B.V. All rights reserved.

PACS: 61.20.Ja; 61.20.Lc; 64.70.Pf

Keywords: Lennard–Jones glass; Molecular dynamics; Supercooled liquid; Relaxation

## 1. Introduction

The understanding of glassy relaxation dynamics is an issue of major concern in condensed matter. In this context, the occurrence of the ubiquitous Kohlrausch stretched

\* Corresponding author. Departamento de Química, Universidad Nacional del Sur (UNS), Av. Alem 1253, Bahía Blanca 8000, Argentina.

E-mail address: [appignan@criba.edu.ar](mailto:appignan@criba.edu.ar) (G.A. Appignanesi).

exponential relaxation law suggested an “heterogeneous” scenario wherein different sub-volumes of the sample relax independently. This description is rooted mainly in the early ideas of Adam and Gibbs [1] that assert the concerted cooperative nature of particle motions.

The existence of “dynamical heterogeneities” in supercooled liquids has been stated both from experimental [2,3] and computational [4–6] standpoints. In this regard, molecular dynamics (MD) simulations provide us with detailed geometrical and dynamical information, since the time evolution of the positions of the particles of moderately large systems can be examined for relatively long times.

In the last years, a series of extensive MD studies of a binary Lennard–Jones system in the supercooled regime determined the fact that “mobile” particles are arranged in clusters [7,8]. Moreover, these global clusters of mobile particles were shown to be built up by a series of quasi-one-dimensional chains of particles termed as “strings”, making evident the correlated nature of particle motion [7]. Additionally, the occurrence of these string-like cooperative motions has been investigated at different temperatures near  $T_c$ , the mode-coupling temperature [7]. These interesting results open the possibility for a mechanistic description of the dynamics and the transport properties of these systems. However, the time evolution of such string-like clusters has not been assessed. The lifetime of the global cluster of mobile particles has been related to the late  $\beta$ -early  $\alpha$  relaxation [8], but the lifetime of the different constituent strings has not been investigated so far. In this work, we shall go beyond the static picture of strings developed in previous works since we shall focus on the detailed time evolution of strings which will be characterised both geometrically and dynamically. This dynamical study has never been performed before and will enable us to demonstrate the highly cooperative nature of the motions of the particles comprised by each string. Also, we shall see that at low  $T$  each string occurs within its own and distinctive sharp time window, independent of the others. Moreover, we shall demonstrate that this localised behaviour is only exhibited at low  $T$  since, as  $T$  increases the different strings evolve during an increasing fraction of the whole characteristic time of the global clusters. Indeed, we shall show that for temperatures around  $T=0.55$  the lifetimes of the strings and of the global clusters of mobile particles become comparable.

## 2. Model and simulation details

The binary Lennard–Jones system we shall employ in our MD simulations has been extensively studied by a series of authors [7–18]. Besides MD studies, this system has also been investigated within the inherent structure formalism of Stillinger and Weber [11–18]. It consists of a three-dimensional mixture of 80% of A and 20% of B particles, the size of the A particles being 10% larger than the B ones. The particles interact by a Lennard–Jones potential characterised by:

$$V(r) = 4\varepsilon \left[ \left( \frac{\sigma}{r} \right)^{12} - \left( \frac{\sigma}{r} \right)^6 \right] \quad (1)$$

with  $\varepsilon_{AA} = 1.0$ ,  $\sigma_{AA} = 1.0$ ,  $\varepsilon_{AB} = 1.5$ ,  $\sigma_{AB} = 0.8$ ,  $\varepsilon_{BB} = 0.5$  and  $\sigma_{BB} = 0.88$ . The interaction potential was truncated at  $r = 2.5 \sigma_{AA}$ . This system has been found not

to crystallise and behaves as a “fragile” glass former. All quantities will be given in dimensionless units involving the Lennard–Jones parameters of the A particles. The system was equilibrated at a series of temperatures for times much longer than the ones required for the correlation functions to decay to zero [10] and long runs were performed to gather the results. We employed the NPT ensemble with a step size of 0.0025, but the results should not depend on whether the NPT or NVE ensemble is used [11]. The total number of particles we used was  $N = 500$ , but we found essentially the same results for larger system sizes. Moreover, the mean square displacement (MSD) curves, the curves for the non-gaussian parameter and the percentage of mobile particles together with the percentage of them involved in strings were consistent with the results of Ref. [7] where 8000 particles were employed. The MSD plots show the typical ballistic, caging localisation, as denoted by a plateau, and diffusive regimes [9,8]. The extent of the plateau depends strongly on temperature, increasing considerably as the mode-coupling temperature,  $T_c$  (estimated at  $0.435^{10}$ ), is approached.

The criterion to identify “mobile” particles [7,8] was to find particles with greater mobility than the one predicted by Brownian dynamics. Particles of enhanced mobility are identified by comparing the self part of the van Hove correlation function  $G_s(r, t)$  with the gaussian function  $G_s^\circ(r, t)$  that measures the probability distribution of a Brownian particle to be located at a distance  $r$  from the origin at time  $t$  [7,8]. Deviation from the gaussian behaviour is measured by the “non-Gaussian parameter”  $\alpha(t)$  [7,8]. The time when  $\alpha(t)$  presents its maximum value,  $t^*$ , defines the time window  $[0, t^*]$  in which the behaviour of the system is most dynamically heterogeneous. The value of  $t^*$  for this Lennard–Jones system depends strongly on temperature as  $T_c$  is approached from above, increasing by almost two orders of magnitude from  $T = 0.55$  to  $0.45$  [7,8]. The height of the maximum in  $\alpha(t)$ ,  $\alpha(t^*)$ , also increases as  $T$  decreases [7,8]. It has been argued that  $t^*$  constitutes a characteristic time for the system under study (interestingly, the curves of the normalised  $\alpha(t)$  for different temperatures collapse when time is scaled by  $t^*$  [8]) and was found to correspond to times in the late  $\beta$ -early  $\alpha$  relaxation (the transition from localised to diffusive behaviour) and to the lifetime of the global clusters of mobile particles [8].

### 3. Time evolution of string-like clusters

We performed many MD simulation runs after equilibration for each of a series of temperatures. We determined the time  $t^*$  for each temperature and for each run we identified the mobile particles as the ones whose displacement at time  $t^*$ ,  $\Delta r_i(t^*) = r_i(t^*) - r_i(0)$  (where  $r_i(t)$  is the position of particle  $i$  at time  $t$ ), was greater than the one predicted by brownian dynamics at such  $T$  (from approximately  $0.6$  to  $0.7\sigma_{AA}$  depending on  $T$  for the range we employed [7,8]). To study the topology of the dynamical heterogeneities present in this system, in particular to find strings of mobile particles, we calculated the distances  $\Delta r_{i,j}(t^*) = r_i(t^*) - r_j(0)$  and recorded the cases when  $\Delta r_{i,j}(t^*) < 0.6$ . This means that after  $t^*$  particle  $j$  has moved and particle  $i$  has occupied its place to within  $0.6\sigma_{AA}$  (in almost all cases when  $\Delta r_{i,j}(t^*) < 0.6$ ,  $\Delta r_{j,i}(t^*) > 0.6$ , which means that the two particles do not interchange positions).

As expected for this system [7,8] we found that 5–10% of the particles, were mobile, independently of temperature. Most of these mobile particles were organised in different strings. The number of mobile particles that participate in strings increased as temperature decreased, as well as the length of the corresponding strings. Most of the

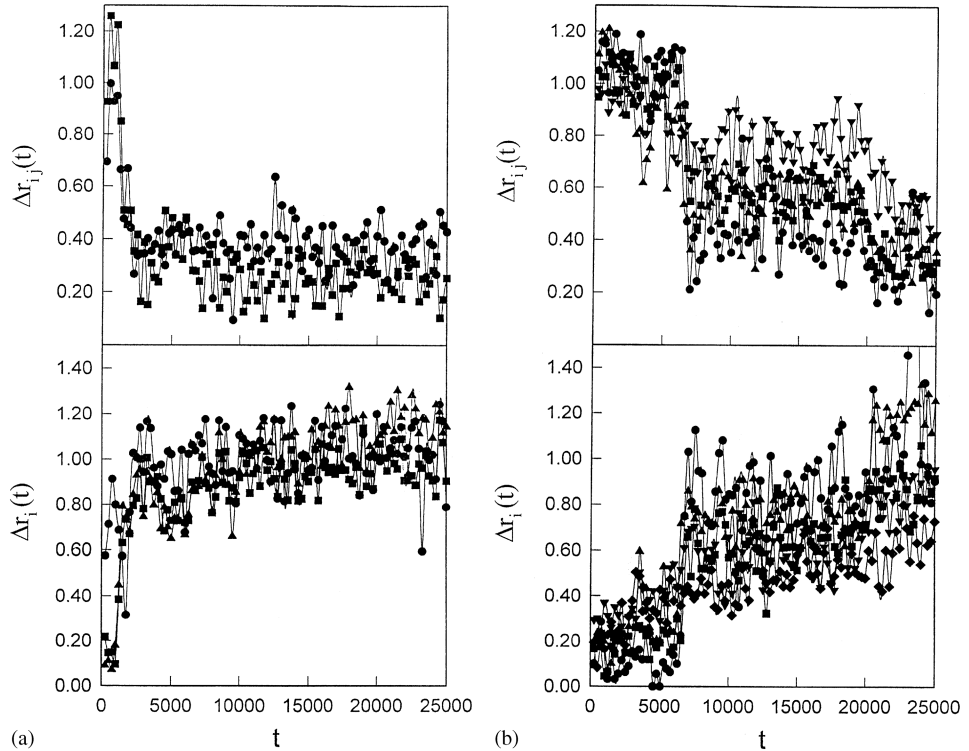


Fig. 1. (a) Time evolution of the five strings ((a)–(e)) of mobile particles of length greater than two (more than two particles involved) found for a run at  $T = 0.469$  (pressure,  $P = 2.296$ , and density,  $\delta = 1.176$ ). (a) Corresponds to the string:  $487 \rightarrow 269 \rightarrow 283$ . Top: Time evolution of  $\Delta r_{i,j}$  (the “bonds”) for the different pairs of  $i$  and  $j$  nearest neighbours of the string. The time axis (as in all figures) is given in MD steps. To read the scale in reduced time, the values must be multiplied by 0.0025, the timestep used. The symbols are as follows:  $\Delta r_{487,269}$ : $\bullet$ ;  $\Delta r_{269,283}$ : $\blacksquare$ ; bottom. Time evolution of the displacements of the particles comprised by the corresponding string,  $\Delta r_i$ .  $\Delta r_{487}$ : $\bullet$ ;  $\Delta r_{269}$ : $\blacksquare$ ;  $\Delta r_{283}$ : $\blacktriangle$ . (b) Same as in (a) but for string:  $435 \rightarrow 324 \rightarrow 37 \rightarrow 327 \rightarrow 226$ . Top.  $\Delta r_{435,324}$ : $\bullet$ ;  $\Delta r_{324,37}$ : $\blacksquare$ ;  $\Delta r_{37,327}$ : $\blacktriangle$ ;  $\Delta r_{327,226}$ : $\blacktriangledown$ ; bottom.  $\Delta r_{435}$ : $\bullet$ ;  $\Delta r_{324}$ : $\blacksquare$ ;  $\Delta r_{37}$ : $\blacktriangle$ ;  $\Delta r_{327}$ : $\blacktriangledown$ ;  $\Delta r_{226}$ : $\blacklozenge$ . (c) Same as in (a) but for string:  $423 \rightarrow 69 \rightarrow 242 \rightarrow 41 \rightarrow 417$ . Top.  $\Delta r_{423,69}$ : $\bullet$ ;  $\Delta r_{69,242}$ : $\blacksquare$ ;  $\Delta r_{242,41}$ : $\blacktriangle$ ;  $\Delta r_{41,417}$ : $\blacktriangledown$ ; bottom.  $\Delta r_{423}$ : $\bullet$ ;  $\Delta r_{69}$ : $\blacksquare$ ;  $\Delta r_{242}$ : $\blacktriangle$ ;  $\Delta r_{41}$ : $\blacktriangledown$ ;  $\Delta r_{417}$ : $\blacklozenge$ . (d) The same as in (a) but for string:  $406 \rightarrow 448 \rightarrow 51$ . Top.  $\Delta r_{406,448}$ : $\bullet$ ;  $\Delta r_{448,51}$ : $\blacksquare$ ; bottom.  $\Delta r_{406}$ : $\bullet$ ;  $\Delta r_{448}$ : $\blacksquare$ ;  $\Delta r_{51}$ : $\blacktriangle$ . (e)  $\Delta r_{i,j}$  for the ramified string:

$$446 \rightarrow 190 \rightarrow 490$$

↓

$$497 \rightarrow 72 \rightarrow 202 \rightarrow 195 \rightarrow 369 \rightarrow 227 \rightarrow 463 \rightarrow 161.$$

Top. Full ramified string; middle. substring:  $446 \rightarrow 190 \rightarrow 490$ ; bottom.  $497 \rightarrow 72 \rightarrow 202 \rightarrow 195 \rightarrow 369 \rightarrow 227 \rightarrow 463 \rightarrow 161$ .

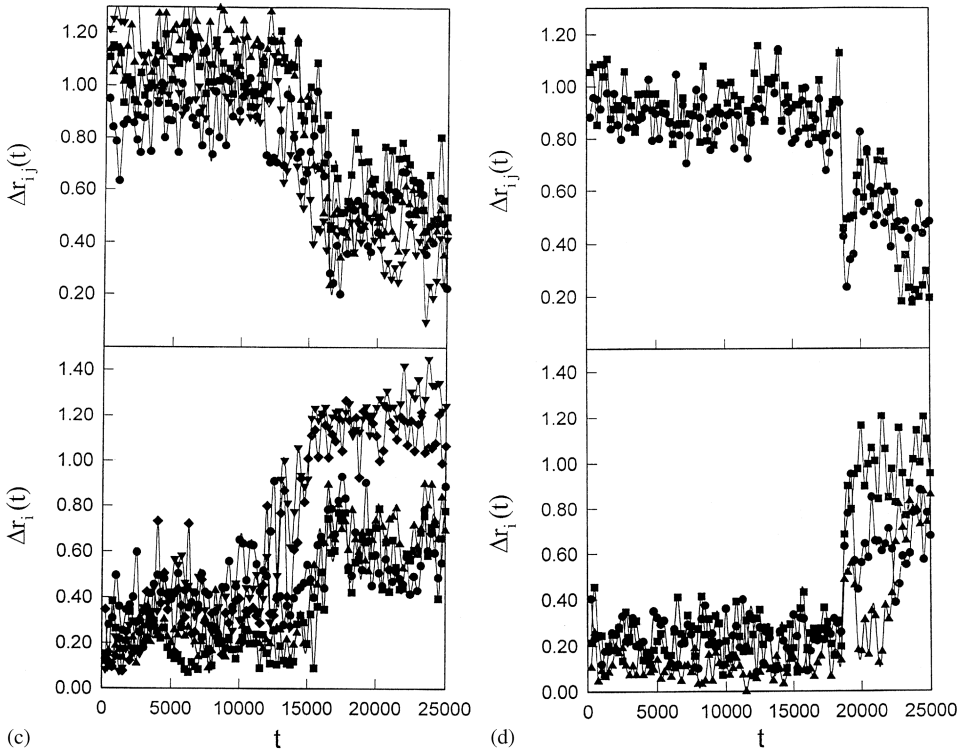


Fig. 1. Continued.

strings found were linear (in the sense they do not present ramifications) and can be represented as  $A \rightarrow B \rightarrow C \rightarrow D \dots$  (which implies that the original position of particle D is occupied by particle C, which is in turn replaced by particle B, and so on). Some cases of simple ramified strings (for example in the form:  $A \rightarrow B \rightarrow C$  together with  $B \rightarrow D \rightarrow E$ ) and very few changes in direction in linear strings (as in  $A \rightarrow B \leftarrow C \rightarrow D$ ) were found and could be described in terms of interaction between (sub)strings (as will be shown later for an example of ramified string). This directional analysis of the strings has not been performed previously and may indicate that string-like cooperative motion can be rationalised as the diffusion (in the opposite direction as the one indicated by the “directional bonds” of the string) of a local inhomogeneity which gives birth to the string (like a hole or local fluctuation, depletion of density). Fig. 1 illustrates these findings for a particular run at  $T = 0.469$  where the different strings found are indicated. The enumeration procedure employed for the particles was such that particles with numbers from 1 to 400 are of type A, while the rest are of type B.

Regarding the “composition” of strings, roughly 30% of the particles that take part in strings are of type B (this percentage is only slightly higher than the percentage of B particles in the whole mixture: 20%). More interesting is the distribution of B

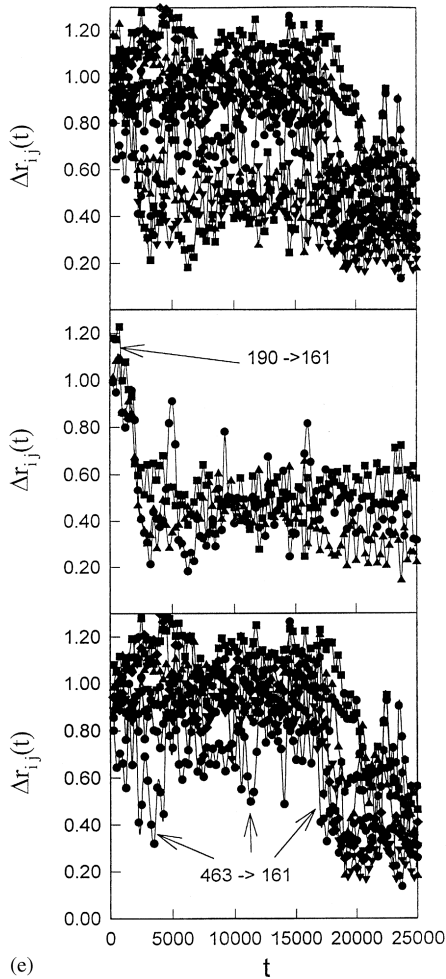


Fig. 1. Continued.

particles amongst the different regions of the strings. We found that most of the B particles that take part in strings are located at the extremes of the strings (the first or the last position of the string). Moreover, roughly half the number of extremes of all the strings studied were occupied by B particles. This fact is quite interesting since the extremes of the strings may be related to the initiation and termination events of the string-like motions (we shall see later on that strings excitations are fast processes once initiated and that the last particles of the strings show a tendency to begin the movement). That the smaller B particles occupy positions related to the initiation events of string motions is not surprising since they would require smaller “holes” (or local fluctuations of density) to move in (however, recall that given the parameters of the Lennard–Jones potential, particularly the values of  $\sigma_{AB}$  and  $\varepsilon_{AB}$ , considerations based

only on the volume of the particles may not hold straightforwardly). Further work is needed to rationalise these results better.

The definition of string used is static in the sense that only the positions of particles at times 0 and  $t^*$  are involved in the computation. To study the time evolution of the strings we calculated the distance between first neighbours in each string as a function of time. This means that for a pair of first neighbours in the string,  $A \rightarrow B$ , we computed the time evolution of the distance  $\Delta r_{A,B}(t) = r_A(t) - r_B(0)$ . This distance evolves from a value greater than  $0.6\sigma_{AA}$  at time  $t = 0$  to a value lower than  $0.6\sigma_{AA}$  at  $t = t^*$  implying that in the time interval  $[0, t^*]$  particle A tends to replace particle B as it moves towards the position first occupied it. Fig. 1 illustrates the time evolution of the strings found for a run at  $T = 0.469$ . An important fact that can be learnt from direct inspection of Fig. 1 is that at this temperature the strings do not evolve throughout the whole time interval  $[0, t^*]$ , but are localised in small time windows, as evidenced by the almost simultaneous sharp drop of the whole set of corresponding distances  $\Delta r_{i,j}$  below  $0.6\sigma_{AA}$  for each string. That is, string-like cooperative motions of particles are highly cooperative short-lived processes (whose lifetime is both much shorter than  $t^*$  and the lifetime of the global cluster of mobile particles). Once a string is established, the corresponding nearest-neighbours distances remain below or oscillating around  $0.6\sigma_{AA}$ . Additionally, another important fact revealed by Fig. 1 is that the different strings do not occur simultaneously, but each one turns out independently at its own different timescale. Previous work on this system indicating the cooperative nature of the motions by means of which the system accomplishes its structural relaxation supported a scenario in the spirit of Adam and Gibbs but in which different sub-volumes or regions of the sample relax not simultaneously but one after other at different timescales [8]. At each time, the relaxing sub-volume is given by the corresponding global cluster of mobile particles which relaxes in a timescale characterised by  $t^*$ , after which the particles comprised are again “caged” [8]. We show now that at low  $T$  the different strings into which each global cluster is decomposed (sub-regions) also relax independently and asynchronously.

Another, but non specific, marker of string-like motion is the time evolution of the displacements of the particles comprised by the string  $\Delta r_i(t) = r_i(t) - r_i(0)$ , where the particle  $i$  belongs to the string under consideration. We can see from Fig. 1 that these quantities show important increments at the time the string-like motion is taking place. The correlated nature of these motions is also apparent from these figures. In spite of the fact that the last particles of each string usually showed a tendency to move first (or to experience large displacements) so as to initiate the corresponding string, string motions do not occur in an stepwise sequential manner (in the sense that each particle performs a complete jump of around  $1\sigma_{AA}$  leaving its place to its left first neighbour which then jumps leaving its place unoccupied, and so on). Instead, the corresponding particles perform important displacements within almost the same time span and the different distances  $\Delta r_{i,j}$  shorten almost simultaneously. This fact is most obvious for short strings, since some long strings can occur in more than one step, a fact that may be explained in terms of interactions between (sub)strings. Fig. 1(e) shows an example of a long string (in this case, a ramified one) that occurs in two well-differentiated cooperative steps (and thus may be decomposed into two substrings).

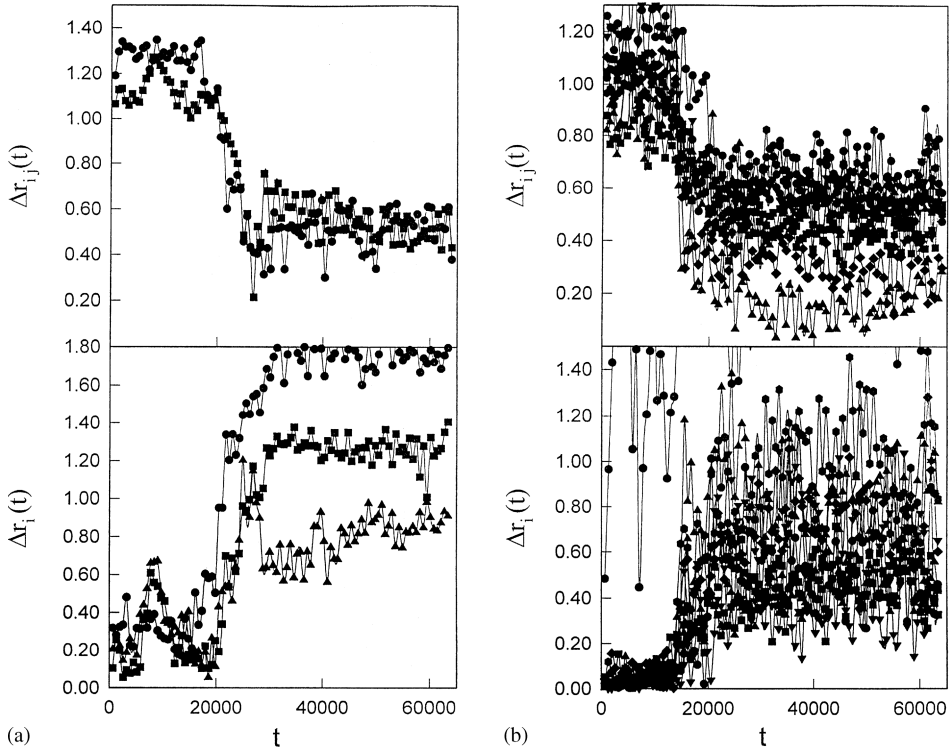


Fig. 2. (a) Typical temperature dependence of the time evolution of the strings from different runs. The time evolution of both  $\Delta r_{i,j}$  and  $\Delta r_i$  are displayed. The symbols that indicate the time evolution of the “bonds” of the strings ( $\Delta r_{i,j}$ ) from left to right, as in Fig. 1, follow the order:  $\bullet$   $\blacksquare$   $\blacktriangle$   $\blacklozenge$ . Also, the symbols that depict the time evolution of the particles that comprise the strings from left to right follow the order:  $\bullet$   $\blacksquare$   $\blacktriangle$   $\blacklozenge$ . (a) Corresponds to  $T = 0.451$  ( $P = 2.680, \delta = 1.191$ ) and to the string:  $209 \rightarrow 88 \rightarrow 365$ . Top. Time evolution of the corresponding values of  $\Delta r_{i,j}$ ; bottom: time evolution of the corresponding values of  $\Delta r_i$ . (b) Same as in (a) for  $T = 0.451$  ( $P = 2.680, \delta = 1.191$ ) but for the ramified string:  $145 \rightarrow 176 \rightarrow 493 \rightarrow 93 \rightarrow 381 \rightarrow 189 \rightarrow 452$



Top. The different  $\Delta r_{i,j}$  as a function of  $t$ ; bottom. The different  $\Delta r_i$  vs.  $t$ . (c) Same as in (a) but for  $T = 0.48$  ( $P = 2.049, \delta = 1.165$ ) and for the string:  $32 \rightarrow 131 \rightarrow 479$ . Top. The different  $\Delta r_{i,j}$  as a function of  $t$ ; bottom. The different  $\Delta r_i$  vs.  $t$ . (d) Same as in (a) but for  $T = 0.48$  ( $P = 2.049, \delta = 1.165$ ) and for the string:  $395 \rightarrow 316 \rightarrow 100 \rightarrow 204$ . Top. The different  $\Delta r_{i,j}$  as a function of  $t$ ; bottom. The different  $\Delta r_i$  vs.  $t$ . (e) Same as in (a) but for  $T = 0.505$  ( $P = 1.477, \delta = 1.140$ ) and for the string:  $336 \rightarrow 238 \rightarrow 290 \rightarrow 366 \rightarrow 412$ . Top. The different  $\Delta r_{i,j}$  as a function of  $t$ ; bottom. The different  $\Delta r_i$  vs.  $t$ . (f) Same as in (a) but for  $T = 0.505$  ( $P = 1.477, \delta = 1.140$ ) and for the string:  $423 \rightarrow 258 \rightarrow 31$ . Top. The different  $\Delta r_{i,j}$  as a function of  $t$ ; bottom. The different  $\Delta r_i$  vs.  $t$ . (g) Same as in (a) but for  $T = 0.55$  ( $P = 0.489, \delta = 1.086$ ) and for the string:  $452 \rightarrow 76 \rightarrow 252$ . Top. The different  $\Delta r_{i,j}$  as a function of  $t$ ; bottom. The different  $\Delta r_i$  vs.  $t$ . (h) Same as in (a) but for  $T = 0.55$  ( $P = 0.489, \delta = 1.086$ ) and for the string:  $194 \rightarrow 327 \rightarrow 463$ . Top. The different  $\Delta r_{i,j}$  as a function of  $t$ ; bottom. The different  $\Delta r_i$  vs.  $t$ .



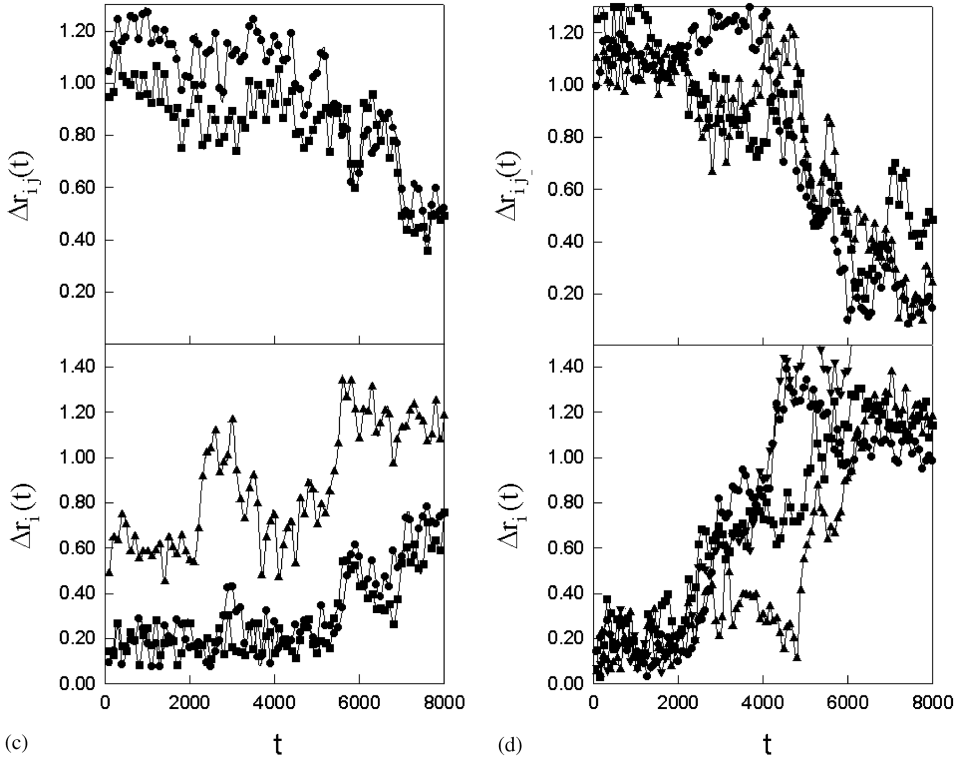


Fig. 2. Continued.

Particle 161 seems to be the one that initiates both substrings. At  $t \sim 2000$  the substring composed of  $446 \rightarrow 190 \rightarrow 490$  occurs. Then, the displacement of particle 161 oscillates (sometimes separating from the former position of 190 farther than  $0.6\sigma_{AA}$ ) and at  $t \sim 17000$  promotes the substring  $497 \rightarrow 72 \rightarrow 202 \rightarrow 195 \rightarrow 369 \rightarrow 227 \rightarrow 463$  while simultaneously approaches again the former position of 190 and thus the whole string is established.

We also studied the effect of temperature on the time evolution of strings. Fig. 2 depicts the time evolution of typical strings at different temperatures ( $T = 0.451, 0.480, 0.505, 0.550$ ) within the corresponding time interval  $[0, t^*]$ . This figure points out the fact that as  $T$  increases the establishment of each string involves an increasing fraction of time  $t^*$ . Indeed, at  $T = 0.55$  the development of each string comprises almost the whole corresponding time interval  $[0, t^*]$ . Thus, Fig. 2 indicates that for temperatures around  $T = 0.55$  the lifetime of string motions and the value of the characteristic time  $t^*$  (and thus, the lifetime of the global clusters) become comparable. This increment in the lifetime of strings is relative to  $t^*$ , since the mean lifetime of a string motion is fairly independent of  $T$  in real terms. We must note that  $t^*$  reduces in almost two orders of magnitude from  $T = 0.451$  to  $T = 0.55$  (see the timescale of the figures) and that the

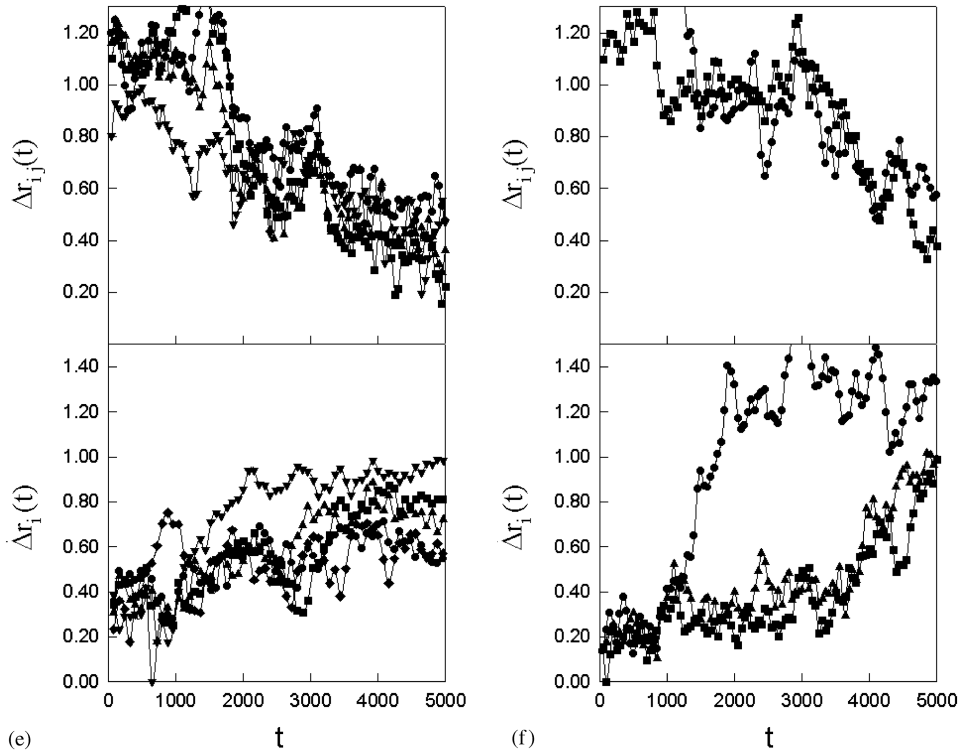


Fig. 2. Continued.

height of the maximum in  $\alpha(t)$ ,  $\alpha(t^*)$ , decreases around seven times, both parameters becoming negligibly small for temperatures higher than  $T = 0.55$ . Concurrently, the plateau in the corresponding MSD plot begins to disappear. These points indicate the fact that for temperatures just above  $T = 0.55$  the behaviour of the system loses the dynamically heterogeneous nature characteristic of lower temperatures and makes the analysis in terms of strings no longer suitable.

#### 4. Concluding remarks

We have geometrically and dynamically characterised the string-like motions that occur in a binary Lennard–Jones system at temperatures close to its mode-coupling temperature. The connectivity and the direction of the bonds in the strings have been indicated. The strings have been shown to take place in a cooperative concerted manner (and not in a sequential stepwise way), as indicated by the concurrent coordinated displacements of the particles involved.

Concerning the influence of temperature on string evolution, we have demonstrated that at low  $T$  the strings evolve within a sharp time window in between the time

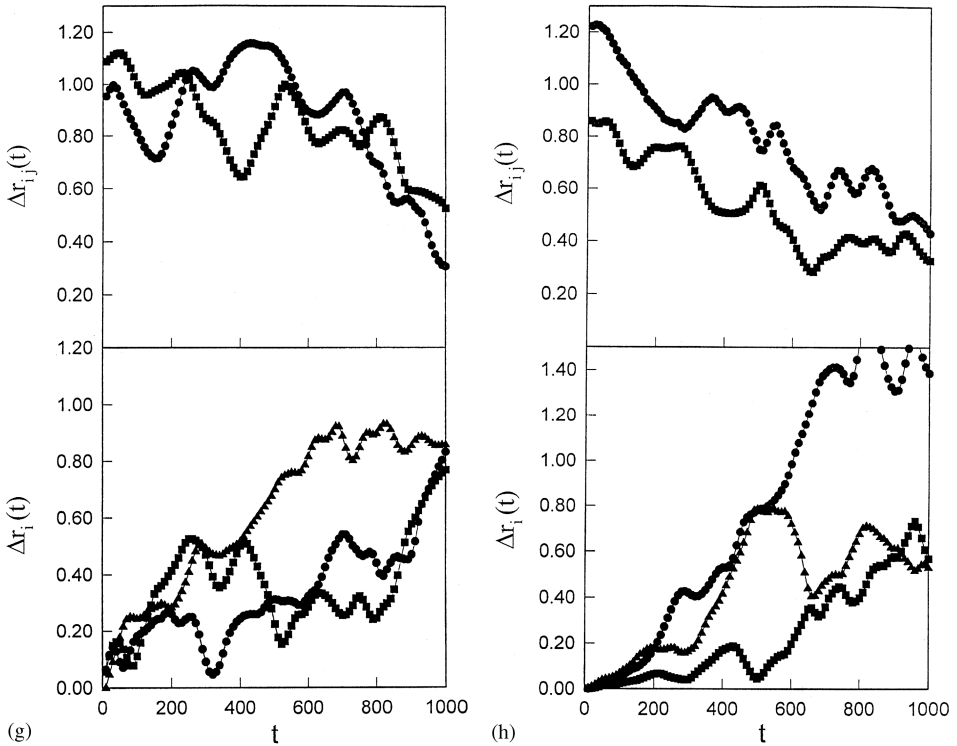


Fig. 2. Continued.

interval  $[0, t^*]$ . Additionally, we showed that the different strings comprised by the global cluster of mobile particles are not correlated in time but occur asynchronously, each at a different time. This fact supports an heterogeneous scenario for the relaxation dynamics but in which the different subregions or clusters of particles relax independently at different timescales. We also revealed the fact that the strings evolve during an increasing fraction of the  $[0, t^*]$  time interval as  $T$  is raised. Moreover, our results indicate that at  $T \sim 0.55$ ,  $t^*$  matches the time span of the events that give rise to the strings. Thus, the lifetimes of the strings and of the global clusters of mobile particles become similar at such temperature.

### Acknowledgements

Financial support from Fundaci3n Antorchas, Consejo Nacional de Investigaciones Cientificas y T3cnicas (CONICET) and the Comisi3n de Investigaciones Cientificas de la Provincia de Buenos Aires (CIC) is gratefully acknowledged. G.A.A. is research fellow of CONICET and R.A.M. is research fellow of CIC.

**References**

- [1] G. Adam, J.H. Gibbs, *J. Chem. Phys.* 43 (1965) 139.
- [2] K. Schmidt-Rohr, H.W. Spiess, *Phys. Rev. Lett.* 66 (1991) 3020.
- [3] M.T. Cicerone, F.R. Blackburn, M.D. Ediger, *J. Chem. Phys.* 102 (1995) 471.
- [4] W. Kob, C. Donati, S.J. Plimpton, P.H. Poole, S.C. Glotzer, *Phys. Rev. Lett.* 79 (1997) 2827.
- [5] A. Heuer, K. Okun, *J. Chem. Phys.* 106 (1997) 6176.
- [6] M. Hurley, P. Harrowell, *Phys. Rev. E* 52 (1995) 1694.
- [7] C. Donati, J.F. Douglas, W. Kob, S.J. Plimpton, P.H. Poole, S.C. Glotzer, *Phys. Rev. Lett.* 80 (1998) 2338.
- [8] C. Donati, S.C. Glotzer, P.H. Poole, W. Kob, S.J. Plimpton, *Phys. Rev. E* 60 (1999) 3107.
- [9] W. Kob, *J. Phys.: Condens. Matter* 11 (1999) R85, and references therein.
- [10] W. Kob, H.C. Andersen, *Phys. Rev. Lett.* 73 (1994) 1376.
- [11] S. Sastry, P.G. Debenedetti, F.H. Stillinger, *Nature* 393 (1998) 554.
- [12] C. Donati, F. Sciortino, P. Tartaglia, *Phys. Rev. Lett.* 85 (2000) 1464.
- [13] P. Debenedetti, F.H. Stillinger, *Nature* 410 (2001) 259, references therein.
- [14] S. Büchner, A. Heuer, *Phys. Rev. E* 60 (1999) 6507.
- [15] F. Sciortino, W. Kob, P. Tartaglia, *Phys. Rev. Lett.* 83 (1999) 3214.
- [16] F. Sciortino, P. Tartaglia, *Phys. Rev. Lett.* 86 (2001) 107.
- [17] S. Sastry, *Nature* 409 (2001) 164.
- [18] J.P. Doye, D.J. Wales, *J. Chem. Phys.* 116 (2002) 3777.